

Dominant resonant mode damping of a piezoelectric tube nanopositioner using optimal sensorless shunts

Sumeet S. Aphale, S. O. Reza Moheimani* and Andrew J. Fleming

Abstract—Piezoelectric tube scanners are used in most commercial scanning probe microscopes, to provide precise motion to the scanning tip. Due to their mechanical construction, they have a relatively low-frequency first resonant mode. This mode gets excited due to environmental noise and introduces errors in the scan obtained. In precision scanning applications, this limits the upper bound of a triangular scan rate to around 1/100th the first mechanical resonance frequency. Feedback control techniques and shunt damping methods have shown promising results in damping this resonant mode and improving scan performance. Most of these techniques need a sensor, which in turn adds complexity to the overall system. With this motivation, *passive* sensorless shunt damping has been investigated and documented. In this work, we design *active* sensorless shunts, optimized using H_2 and H_∞ techniques. These shunts damp the modal amplitude of the first resonant peak by almost 24 dB. A triangle raster pattern used to test the scan accuracy shows significant improvement due to the damping achieved by these active shunts.

I. INTRODUCTION

Increasing demands on the scanning precision achieved by electron microscopes led to the development of Scanning tunneling microscopes (STM) and atomic force microscopes (AFM) [1], [2]. In a typical STM, a scan is obtained by sensing and outputting the tunneling current to the control station while the sample is held stationary and the piezoelectric tube scanner scans a sharp metallic probe over the sample surface in a raster pattern [3]. STMs and AFMs are an indispensable part in nanotechnology research. With nanotechnology applications in such areas as nanoelectronics, medicine, biotechnology, national security, cell biology, micro-machining, particle physics and sub-atomic chemistry increasing by the day [4], [5], [6], [7], [8], STMs and AFMs with better scan performance are being demanded [9], [10]. Upcoming applications require the STMs and AFMs to have higher scan speeds and accuracy. This has in turn, generated significant interest in the area of precision motion at the nanometer and sub-nanometer scales.

High resolution, greater repeatability, mechanical simplicity and greater bandwidth offered by piezoelectric tube scanners, make them ideal for such high precision applications. Mechanical simplicity and ease of integrability into microscopes and precision motion systems make piezoelectric tube scanners ideal for scanning tunneling microscopes, atomic

force microscopes, nanomachining, etc. Tube scanners with a large length/diameter ratio are known to have improved deflection sensitivity and a larger deflection range. The direct consequence of such designs with large length/diameter ratio is a low mechanical resonance frequency. This mechanical resonance can be inadvertently excited by harmonic components of the input motion signal and thus produce unwanted vibrations. These vibrations introduce spurious motions that result in inaccurate scans. Left unchecked they can lead to the gradual deterioration and ultimate destruction of the scanner. These vibrations are, therefore, a main cause of concern when piezoelectric tube scanners are utilized for nanopositioning applications and effective techniques that impart damping to the resonant modes are sought after.

To alleviate the problems caused by these resonant modes, feedback control and shunt damping techniques have been applied [11], [12], [13], [14]. These techniques have shown to augment the system damping substantially. Sensors are required to implement either of these damping techniques. This can make the control strategy expensive and the required mechanical apparatus bulky. The introduction of an external sensor also increases system complexity. Additional power needed for the sensor has to be addressed. Signal processing issues such as sensor bandwidth, sensor noise and sensor calibration also have to be dealt with. Thus, it is beneficial to achieve damping without the use of an external sensor. With this motivation, the idea of sensorless shunt damping has been investigated.

In [15], the implementation of *passive* sensorless shunt damping is reported. There, an LRC impedance is connected to the piezoelectric transducer. When subject to deflection, the charge generated in the transducer flows through the external (shunt) impedance developing a counteractive voltage across the terminals, thus damping the vibrations. Due to the inherent redundancy, sensorless shunt damping can be implemented independently or in conjunction with an existing technique to improve scan performance. Passive shunts need external circuitry to be attached to one of the electrodes. The use of synthetic impedances for piezoelectric shunt damping has been explored [16], [17]. Most commercially available STMs have their own control units that are redundant enough for the synthetic implementation of active shunts for damping, and perform the remaining tasks needed for a smooth STM operation. This paper presents new results on *active* sensorless shunts optimally designed using H_2 and H_∞ techniques for a piezoelectric tube nanopositioner.

Section II gives a brief introduction to the mechanical construction and the basic operation of a piezoelectric tube

This work was supported by the Australian Research Council's Center for Complex Dynamic Systems and Control

Authors are with School of Electrical Engineering and Computer Science, University of Newcastle, Callaghan NSW 2308, Australia (sumeet.aphale, andrew.fleming, reza.moheimani) @newcastle.edu.au

* Corresponding author

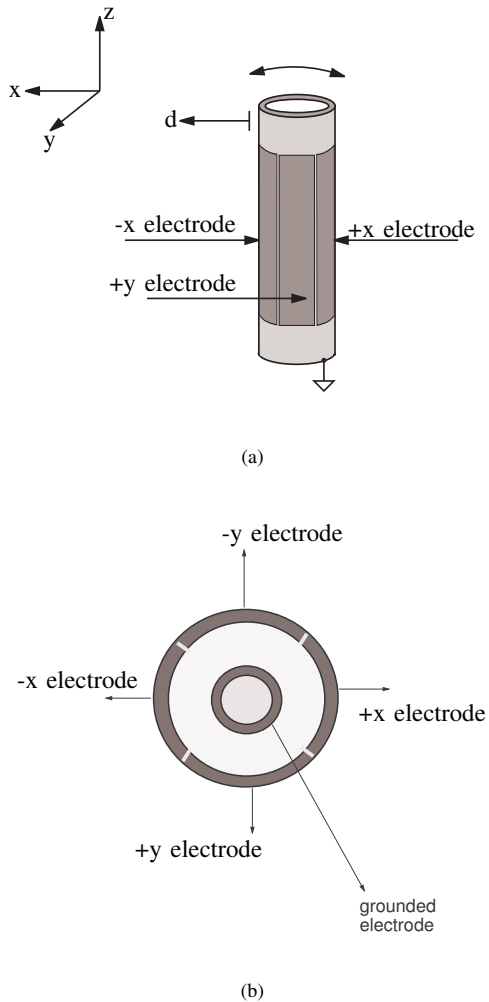


Fig. 1. (a) Side-view and (b) top-view of a piezoelectric tube nanopositioner.

scanner. Section III describes the experimental setup used in this work. The details of the system identification and the simulated shunt damping results are also presented. Experimental results along with a comparison of the damped vs the undamped performance of the piezoelectric tube scanner with respect to a raster scan pattern, will follow in Section IV. Section V gives the conclusions and contributions.

II. PIEZOELECTRIC TUBE SCANNER

A typical STM consists of three main parts: the scanning head which houses the piezoelectric tube scanner and the preamplifier circuit, the base on which the sample to be scanned is mounted and the support system which lends support to both the head and the base [18]. All STMs also have a control unit which controls the motion of the scanning tip and collects and collates the scan data to produce an image of the scanned sample. The piezoelectric

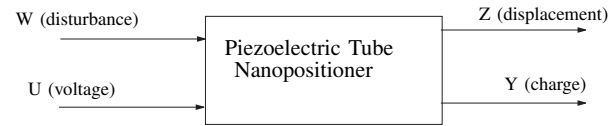


Fig. 2. Two-input two-output equivalent block diagram for the piezoelectric tube nanopositioner

tube nanopositioner is the most important part of an STM system.

Figure 1(a) shows the main components of a typical tube nanopositioner. It is a tube made of radially poled piezoelectric material that has four external electrodes and a grounded internal electrode, see Figure 1(b). Motion along a single axis is controlled by two opposing electrodes (-x and +x for x axis) and (-y and +y for y axis) [19]. This configuration minimizes the horizontal and vertical coupling between the two perpendicular axes and accurate motion in each individual axis is possible. It is this simplicity in construction that makes the piezoelectric tube scanner an actuator of choice in scanning probe microscopy.

In a typical STM, the piezoelectric tube scanner is used as a nanopositioning platform on which the sample is placed while a micro-cantilever is used to scan the sample by moving the piezoelectric tube scanner in the X-Y plane and the micro-cantilever in the Z direction. The scans are obtained by tracing a raster-type pattern, where one axis gets a triangle wave input and the other gets a ramp type input. The high frequency components of this input triangle wave as well as the ambient noise can excite the dominant first resonant mode of a piezoelectric tube scanner and reduce the accuracy of the obtained scan. Thus, damping the first resonant mode of the piezoelectric tube scanner is extremely important. Using the basic principles of piezoelectric shunt damping [20], [21], this paper will describe a novel way of damping the resonant mode by implementing optimal sensorless shunts.

III. SYSTEM MODELING AND SIMULATIONS

Identifying the actual transfer functions between inputs and outputs of interest and fitting a fairly accurate model to the identified system, is the first step in this work. The piezoelectric nanopositioner is treated as a two-input two-output system. A simple block diagram of the two-input two-output system is given in Figure 2. A detailed schematic of the piezoelectric tube nanopositioner with all the inputs and outputs is given in Figure 3. Note that the capacitive sensor is used purely to measure the displacement (either for system identification or for determining the accuracy of the scan performance, as mentioned in Section IV) and does not actively feature in the resonant mode damping technique described in this work.

A. Modeling

In this case, Z and Y represent the outputs displacement and charge respectively and W and U are the inputs, distur-

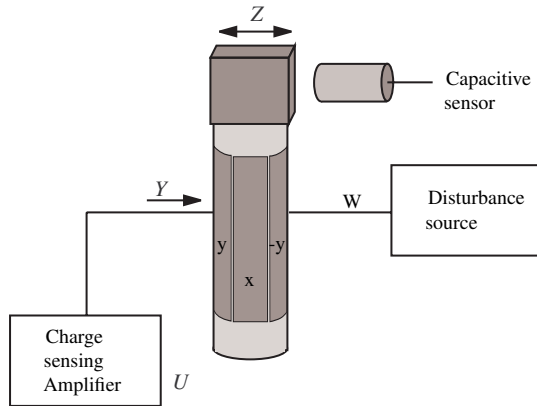


Fig. 3. Schematic diagram denoting the inputs and outputs of the tube scanner

bance and voltage. The frequency response function (FRF) $G_{ij}(j\omega)$ is a 2×2 matrix where each element $G_{ij}(j\omega)$, $i, j = 1$ and 2 , corresponds to a particular combination of the input and the output (for example $G_{YW}(j\omega) = Y(j\omega)/W(j\omega)$ when $U = 0$). These FRFs are determined by applying a sinusoidal chirp of varying frequency (from 10 Hz-1.2 KHz) as inputs (W and U) to the corresponding piezoelectric actuators and measuring the output signals (Y and Z). This frequency range was chosen as there are no dominant low frequency dynamics that need to be considered during shunt design and it captures the first resonant mode of the piezoelectric tube scanner.

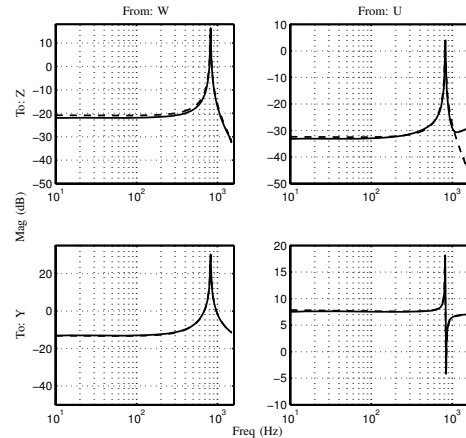
Mathematically, the system can be described as:

$$\begin{bmatrix} Z \\ Y \end{bmatrix} = \begin{bmatrix} G_{ZW}(s) & G_{ZU}(s) \\ G_{YW}(s) & G_{YU}(s) \end{bmatrix} \begin{bmatrix} W \\ U \end{bmatrix}.$$

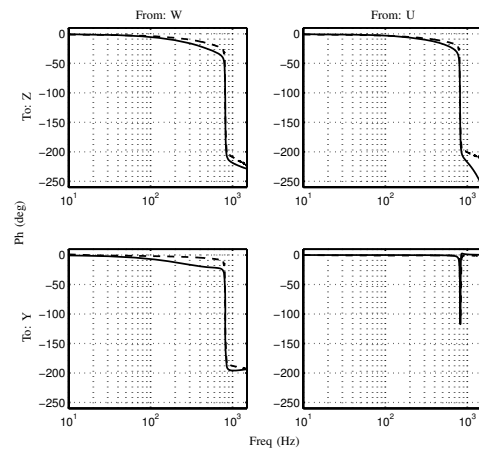
A subspace based modeling technique is used to procure an accurate model of the experimental system [22]. Figure 4 illustrates the measured two-input two-output frequency responses of the system as well as the identified model. The inputs are voltage (in V) and disturbance (in μm) while the outputs are charge and displacement. The charge is measured (in μC) using a charge sensing amplifier while the displacement is measured (in μm) using a capacitive sensor. A second order model is obtained using the sub-space based algorithm, to fit the measured transfer functions, to reduce complexity. The fit is simple and captures the system dynamics fairly accurately.

B. Design and simulation of active sensorless shunts

Once the four transfer functions are identified and modeled accurately using a second order model approximation, the problem reduces to finding an optimal regulator. A schematic of a typical H_2 or H_∞ optimization problem is shown in Figure 6. P is the plant under consideration, u_1 and u_2 are the inputs and y_1 and y_2 are the respective outputs. K is a controller (either H_2 or H_∞) that stabilizes the



(a)



(b)

Fig. 4. Magnitude and Phase response of the actual (—) and the modeled (- -) two-input two-output tube nanopositioner system.

plant and minimizes the respective norm between the disturbance and the weighted output. In terms of the piezoelectric nanopositioner, this equates to finding a controller for the transfer function between output charge and input voltage G_{YU} such that the norm between input disturbance W and output displacement Z is minimized. Figure 5 shows the standard implementation of a shunt used to damp resonance in a piezoelectric tube scanner. The principle behind shunt damping is to measure output charge Y and regulate input voltage U (the same principle that the controllers work on) and thus, can be replaced by the controllers designed using the aforementioned techniques. In other words, the optimal H_2 and H_∞ controllers can be implemented as synthetic shunts for damping the low-frequency first resonant mode of the piezoelectric tube scanner.

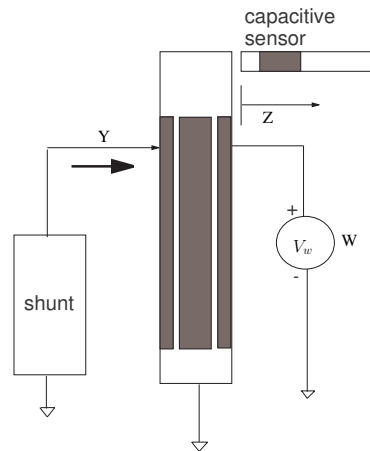


Fig. 5. Shunt implementation for damping resonance in a piezoelectric tube scanner

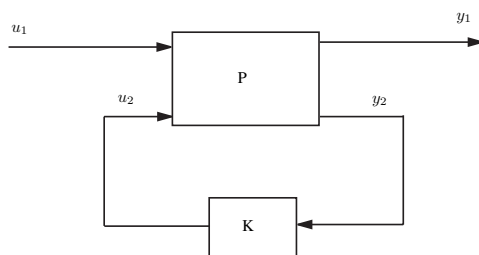


Fig. 6. Schematic of a typical optimization problem

In order to design a shunt controller that is not of excessive gain, the performance output Z is augmented with the control signal multiplied by a weighting function w_t as shown in Figure 7 [23]. Optimal controllers are obtained using both H_2 and H_∞ optimization techniques and the close loop system responses are simulated. These optimally designed controllers are connected to one of the electrode terminals of the tube and thus act as shunts. The frequency responses of these optimized shunts are provided in Figure 8. The shunt performance is tested using simulations. Figure 9(a) presents the experimental results for a H_2 shunt. As can be clearly seen, almost 24 dB damping is obtained. Figure 9(b) presents the experimental results for a H_∞ shunt. This controller achieves almost 25 dB of damping at the resonant mode.

Note that only one of the electrodes is connected to the shunt while the other electrode is used purely to evaluate the performance of the shunted system. The optimized shunt is designed using the frequency response of the system and is shown to provide good damping at the resonant mode of interest. These sensorless piezoelectric shunts are implemented digitally using a dSPACE-DS1103 rapid prototyping system and they provide the necessary damping to the nanopositioner tube system.

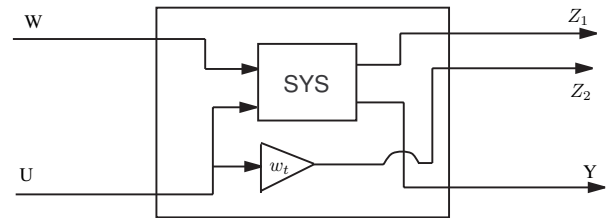


Fig. 7. Schematic of the actual system used in the optimization techniques

IV. EXPERIMENTAL RESULTS

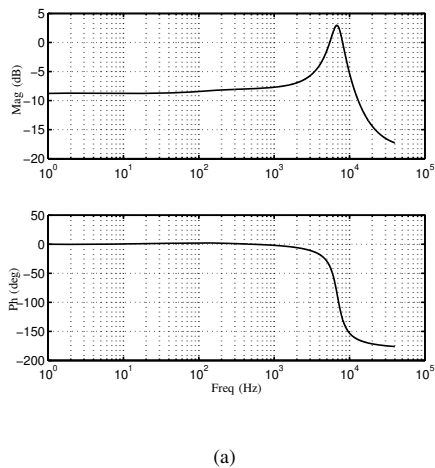
Most piezoelectric tubes have a lightly damped mechanical resonance at relatively low frequencies (in the hundreds of Hz). In precision scanning applications, this limits the upper bound of a triangular scan rate to around 1/100th the first mechanical resonance frequency. This is in the region of 5 Hz-15 Hz for most feasible tube scanner designs. Consequently, good tracking of a 5 Hz triangle wave was presented in [24]. For a better performance over a broader range of frequencies, it is beneficial to damp this resonant mode. To achieve this damping, feedback control techniques and shunt control techniques have been researched, implemented and documented.

A. Active sensorless shunts

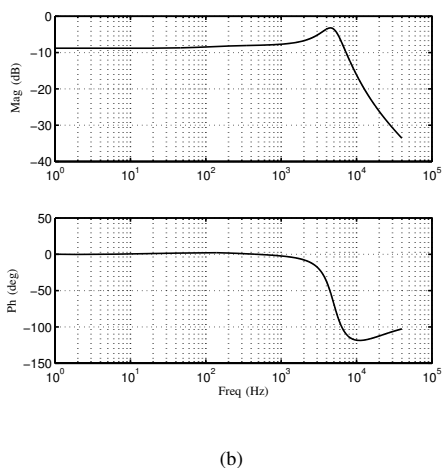
In this work, the feasible inputs and outputs are identified and the shunt design problem is changed into a standard linear regulator design problem. This facilitates the design of robust synthetic shunts using optimization techniques such as H_2 and H_∞ . The performance of this technique is not dependent on sensor resolution as is the case with most feedback control techniques and shunt control methods that are not sensorless. Figures 9(a) and 9(b) clearly show the damping achieved in both the cases by implementing the robust sensorless shunts. The first resonant mode of the piezoelectric tube nanopositioner is damped by almost 24 dB. These shunts are active and can be easily tuned for variations in resonance frequency or to achieve different levels of damping by altering a single optimization parameter in the design code. With the design code built into the control center of the STM, these shunts may prove more manageable (in terms of tuning and adjustments) in practice than their *passive* counterparts. These active shunts exclude the need of a sensor as well as that of any passive components (RLC) which are necessary for their passive counterparts as shown in [15].

B. Evaluation of improvement in scan accuracy

Damping performance of these shunts was tested on a piezoelectric tube scanner that was made to trace a raster pattern [25]. A 1.6 V, 23.5 Hz triangle wave was used as the input signal. The first resonant mode of the tube scanner occurs at 814.6 Hz. The input triangle signal has harmonics which excite this resonance and cause distortions in the traced scan. The super-imposed high-frequency harmonic



(a)



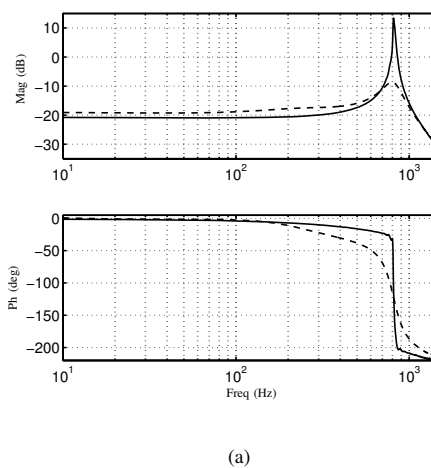
(b)

Fig. 8. Frequency response of the implemented H_2 (a) and H_∞ (b) optimized shunts.

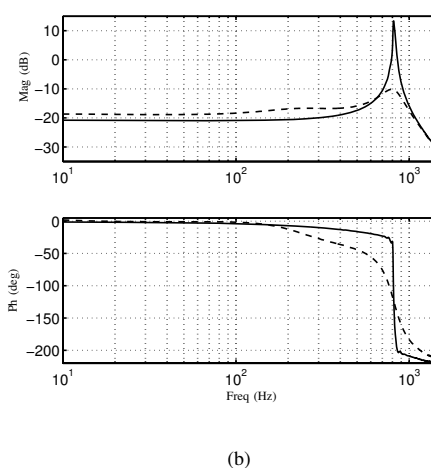
distortion in the traced raster scan is clearly visible, see Figure 10. H_2 and H_∞ shunts damp the resonant peak and the raster is cleaner, thus providing an accurate scan of the sample of interest. The scans traced by the shunt-damped tube scanner show substantial reduction of these distortions. Figure 11 shows the error in 80% of the raster trajectory. The scan traced by the shunt-damped tube scanner shows a reduction of error with respect to that traced by the undamped tube scanner by a factor of 5 (from ± 100 nm for the undamped scan to ± 20 nm for the damped scan).

V. CONCLUSIONS

The first resonant mechanical mode of the piezoelectric tube scanner can be excited by environmental noise or input harmonics which, in turn, introduce errors in the traced raster scans. Damping the resonant mode has the potential to reduce the errors caused by these harmonic distortions. Design of suitable shunts that add sufficient damping to the



(a)



(b)

Fig. 9. (a) Measured undamped (---) and H_2 -damped (—) frequency responses. (b) Measured undamped (---) and H_∞ -damped (—) frequency responses.

tube scanner can be formulated as a standard optimization problem. H_2 and H_∞ optimization techniques can be used to design well-performing active shunts. These shunts are robust, easy to implement and totally eliminate the need for a sensor required in feedback control strategies. These active sensorless shunts damp the first resonant mechanical mode of the piezoelectric tube scanner by 24 dB. This results in a reduction in the scan errors by a factor of five (from $0.1 \mu\text{m}$ by the undamped system to $0.02 \mu\text{m}$ by the damped system).

REFERENCES

- [1] G. Binnig and D. P. E. Smith, "Single-tube three-dimensional scanner for scanning tunneling microscopy," *Review of Scientific Instruments*, vol. 57, no. 8, pp. 1688–1689, August 1986.
- [2] G. Binnig and H. Rohrer, "The scanning tunneling microscope," *Scientific American*, vol. 253, pp. 50–56, 1986.

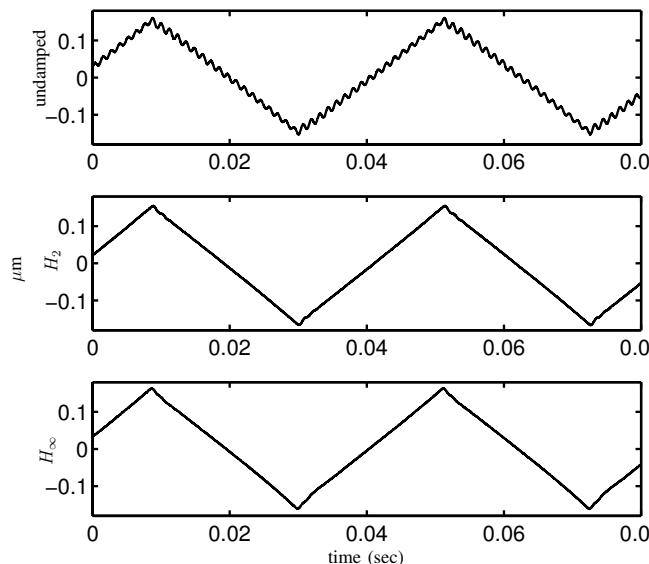


Fig. 10. Undamped raster pattern (—) vs rasters damped using H_2 shunt (\cdots) and H_∞ shunt (- -).

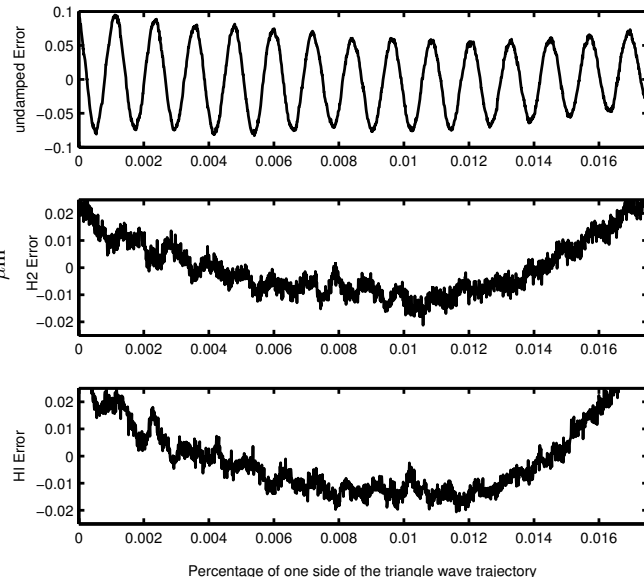


Fig. 11. Plot of deviation from linear in 80% of scan waveform (Note that the undamped deviation is plotted on a scale of $\pm 0.1 \mu\text{m}$ while the damped H_2 and H_∞ deviations are plotted on a scale of $\pm 0.02 \mu\text{m}$).

- [3] L. Libioulle, Y. Houbion, and J.-M. Gilles, "Very sharp platinum tips for scanning tunneling microscopy," *Review of Scientific Instruments*, vol. 66, no. 1, pp. 97–100, 1995.
- [4] I. Fujimasa, *Micromachines: A New Era in Mechanical Engineering*. Oxford, UK: Oxford University Press, 1996.
- [5] M. Scott, "MEMS and MOEMS for national security applications: Reliability, testing and characterization of MEMS/MOEMS II," ser. 4980, SPIE, Bellingham, 2003.
- [6] G. Kovacs, *Micromachined Transducers Sourcebook*. Boston, USA: WCB McGraw-Hill, 1998.
- [7] C. L. P. San and E. P. H. Yap, Eds., *Frontiers in Human Genetics*. Singapore: World Scientific, 2001.
- [8] T. A. Desai, W. H. Chu, J. K. Tu, G. M. Beattie, A. Hayek, and M. Ferrari, "Microfabricated immunisolating biocapsules," *Biotechnology and Bioengineering*, vol. 57, pp. 118–120, 1998.
- [9] G. Schitter, R. W. Stark, and A. Stemmer, "Fast contact-mode atomic force microscopy on biological specimens by model-based control," *Ultramicroscopy*, vol. 100, pp. 253–257, 2004.
- [10] J. Akila and S. S. Wadhwa, "Correction for nonlinear behaviour of piezoelectric tube scanners used in scanning tunneling and atomic force microscopy," *Review of Scientific Instruments*, vol. 66, no. 3, pp. 2517–2519, March 1995.
- [11] D. Croft and S. Devasia, "Vibration compensation for high speed scanning tunneling microscopy," *Review of Scientific Instruments*, vol. 70, no. 12, pp. 4600–4605, December 1999.
- [12] D. Croft, D. McAllister, and S. Devasia, "High-speed scanning of piezo-probes for nano-fabrication," *Transactions of the ASME, Journal of Manufacturing Science and Technology*, vol. 120, pp. 617–622, August 1998.
- [13] N. W. Hagood and A. V. Flotow, "Damping of structural vibrations with piezoelectric materials and passive electrical networks," *Journal of Sound and Vibration*, vol. 146, no. 2, pp. 246–268, 1991.
- [14] N. Tamer and M. V. Dahleh, "Feedback control of piezoelectric tube scanners," in *Proc. IEEE Conference on Decision and Control*, Lake Buena Vista, FL, USA, December 1994, pp. 1826–1831.
- [15] A. J. Fleming and S. O. R. Moheimani, "Sensorless vibration suppression and scan compensation for piezoelectric tube nanopositioners," *IEEE Transactions on Control System Technology*, vol. 14, no. 1, pp. 33–44, 2006.
- [16] A. J. Fleming, S. Behrens, and S. O. R. Moheimani, "Synthetic impedance for implementation of piezoelectric shunt damping circuits," *IEE Electronics Letters*, vol. 36, no. 18, pp. 1525–1526, August 2000.
- [17] A. J. Fleming and S. O. R. Moheimani, "Control oriented synthesis of high performance piezoelectric shunt impedances for structural vibration control," *IEEE Transactions on Control Systems Technology*, vol. 13, no. 1, pp. 98–112, January 2005.
- [18] B. Bhushan, *Handbook of Micro/Nanotribology*, 2nd ed. Boca Raton, USA: CRC, 1999.
- [19] C. J. Chen, "Electromechanical deflections of piezoelectric tubes with quartered electrodes," *Applied Physics Letters*, vol. 60, no. 1, pp. 132–134, January 1992.
- [20] S. Y. Wu, "Method for multiple mode shunt damping of structural vibration using a single pzt transducer," in *SPIE Smart Structures and Materials, Smart Structures and Intelligent Systems*, vol. 3327, March 1998, pp. 159–168.
- [21] J. J. Hollkamp, "Multimodal passive vibration suppression with piezoelectric materials and resonant shunts," *Journal of Intelligent Materials Systems and Structures*, vol. 5, pp. 49–56, 1994.
- [22] T. McKelvy, H. Akcay, and L. Ljung, "Subspace-based multivariable system identification from frequency-response data," *IEEE Transactions on Automatic Control*, vol. 41, pp. 960–979, July 1996.
- [23] J. C. Doyle, K. Glover, P. Khargonekar, and B. Francis, "State-space solutions to standard H_2 and H_∞ control problems," *IEEE Transactions on Automatic Control*, vol. 34, no. 8, pp. 831–847, August 1989.
- [24] S. Salapaka, A. Sebastian, J. P. Cleveland, and M. V. Salapaka, "High bandwidth nano-positioner: A robust control approach," *Review of Scientific Instruments*, vol. 75, no. 9, pp. 3232–3241, September 2002.
- [25] H. Perez, Q. Zou, and S. Devasia, "Design and control of optimal scan trajectories: Scanning tunneling microscope example," *Journal of Dynamic Systems, Measurement, and Control*, vol. 126, pp. 187–197, March 2004.